UV-Assisted Li^+ Catalyzed Free Radical Polymerization of Vinyl Ethers: A New Strategy for Creating Hydrolysis-Resistant and Long-Lived Polymer Brushes As "Smart" Surface Coating

1. EXPERIMENTAL

1.1 Antifouling and Bactericidal Assay.

The construction of the antibacterial brush layer is based on the successful grafting of the surface PVEs brush coating. After tethering PVEs polymer brush, the Si_xN_4-*g*-PHBVE wafer was soaked into PBS solution, 0.1 mol/L NaOH(eq) and 0.1 mol/L HCl(eq) for several weeks. After that, took them out, and then purged in an argon atmosphere for 3 min. Subsequently, the modified Si_xN_4 wafer reacted with GAGs (0.5 g) in DMSO solution (10 g) at 80 °C for 4 hours under the condition of a small amount of NaOH catalyzed. Escherichia coli (ATCC 35218) glycerol stock was streaked on LB agar plates, then, blank and modified Si_xN_4 wafers were lay flat into plates for overnight culture at 37 °C, observing whether there any bacteriostatic rings.

1.2 Surface protein microarray fabrication.

After the well-defined PVEs layer was fixed on BOPP, the target Collins reagent was used as oxidizer to convert -OH to -CHO, further, bovine serum albumin (AF555-IgG) was diluted to 5 μg/mL in PBS solution (pH=7.4) and then spotted (noncontact dispensing) on the functionalized BOPP surface. The prepared microarray was kept at 4 °C for 24 h and measured by a fluorescence to obtain the initial fluorescence signal. After fixed treatment, the microarray was rinsed with washing buffer for 1 h and wished with deionized water five times to remove free protein. Fluorescence signal characterization of the cleaned microarray under the same test conditions, the immobilization efficiency of AF555-IgG was calculated as the ratio of fluorescence intensity before and after washing.

2. RESULTS

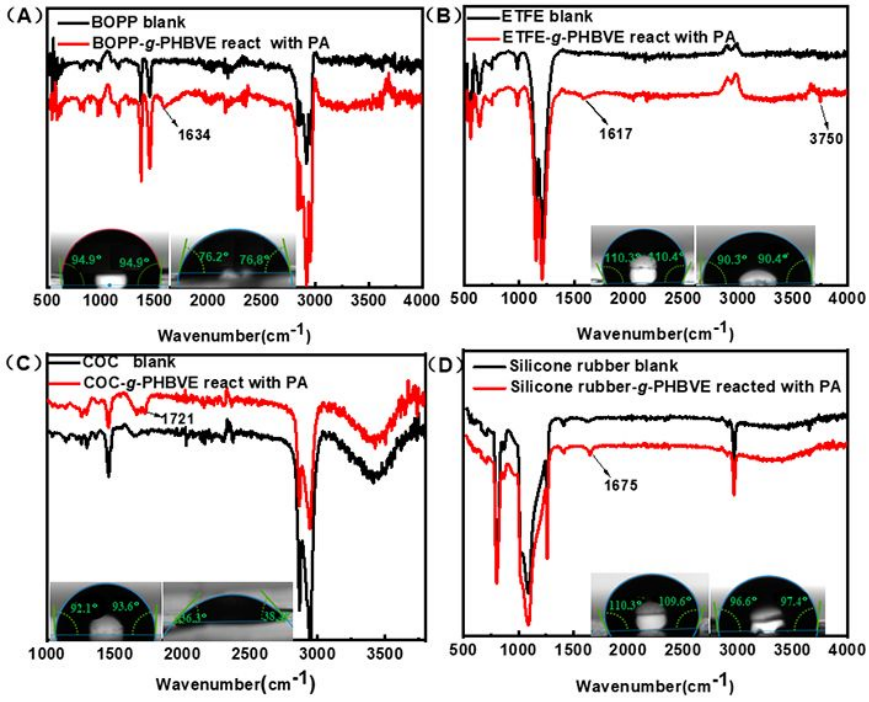

Figure S1. ATR-FTIR and dynamic water contact angle measurements of blank film (black line) and functionalized film (red line), the functionalization process was on BOPP, ETFE, COC, MQ, respectively. After coating with PVEs layer, the film surface changes from hydrophobic to hydrophilic.

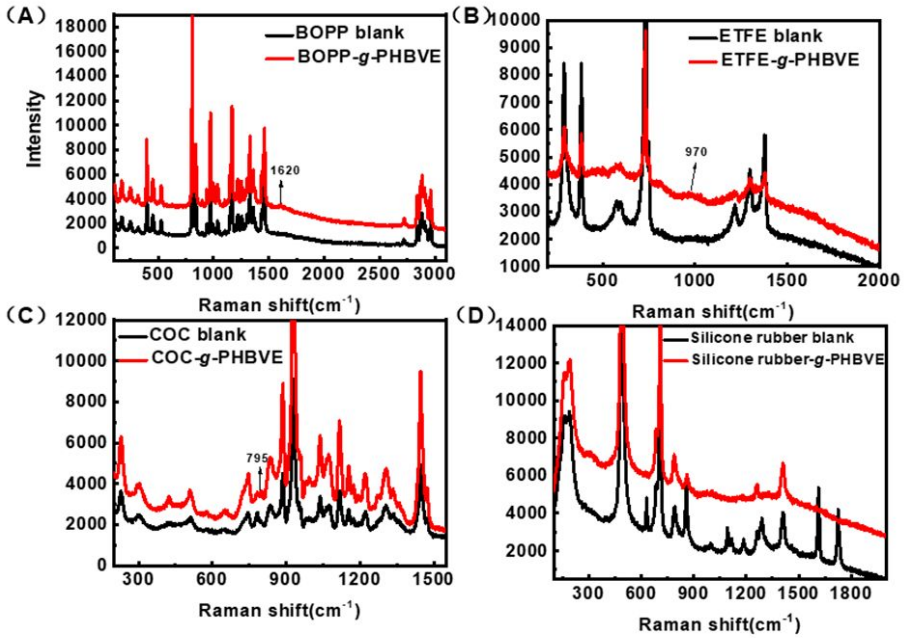

Figure S2. Raman spectroscopy characterization of blank film (black line) and PVEs layer functionalized film (red line). Raman laser was selected as 785 nm, and the scanning band was 400-3500 cm^{-1}.

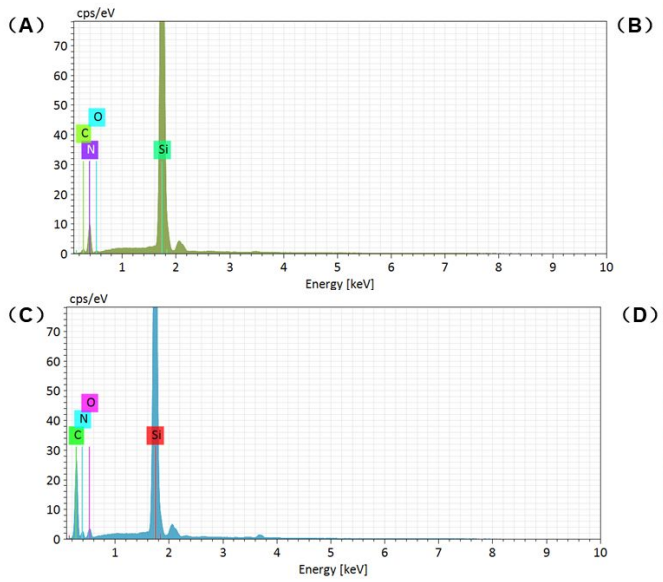

element	Normalized quality [%]	atom [%]
Si	79.34	65.13
N	16.86	27.76
C	3.42	6.57
O	0.37	0.54
	100.00	**100.00**

element	Normalized quality [%]	atom [%]
Si	53.92	33.99
C	38.80	57.20
N	4.79	6.06
O	2.49	2.75
	100.00	**100.00**

Figure S3. EDS spectrograms and element quantitative analysis of (A) blank Si_xN_4; (B) Si_xN_4-*g*-PHBVE.

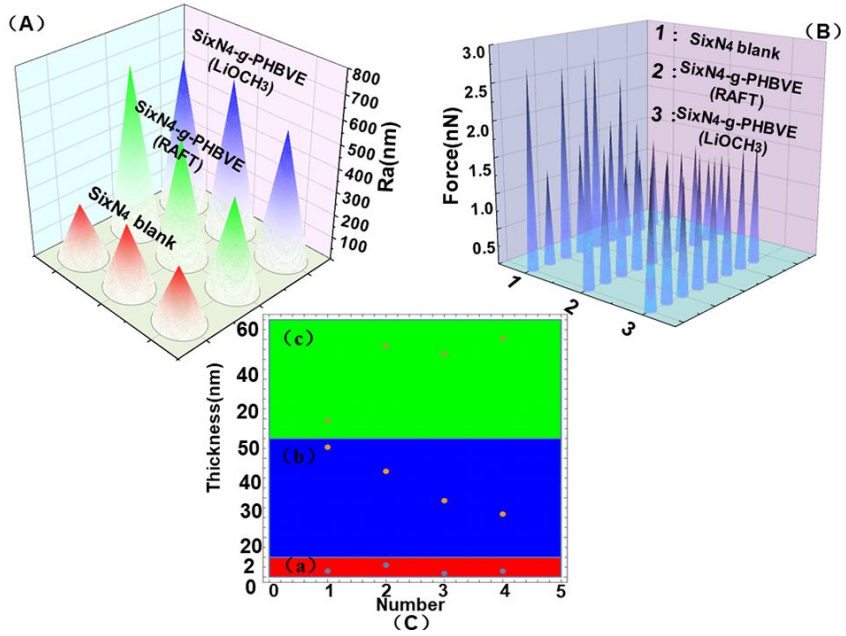

Figure S4. (A) Surface roughness statistics of blank Si_xN_4 (red), Si_xN_4-*g*-PHBVE (RAFT, green), Si_xN_4-*g*-PHBVE (Li^+, blue); (B) Surface adhesion statistics of blank Si_xN_4 (1), Si_xN_4-*g*-PHBVE (RAFT, 2), Si_xN_4-*g*-PHBVE (Li^+, 3); (C) Surface polymer brush thickness statistics of blank Si_xN_4 (a), Si_xN_4-*g*-PHBVE (RAFT, b), Si_xN_4-*g*-PHBVE (Li^+, c).

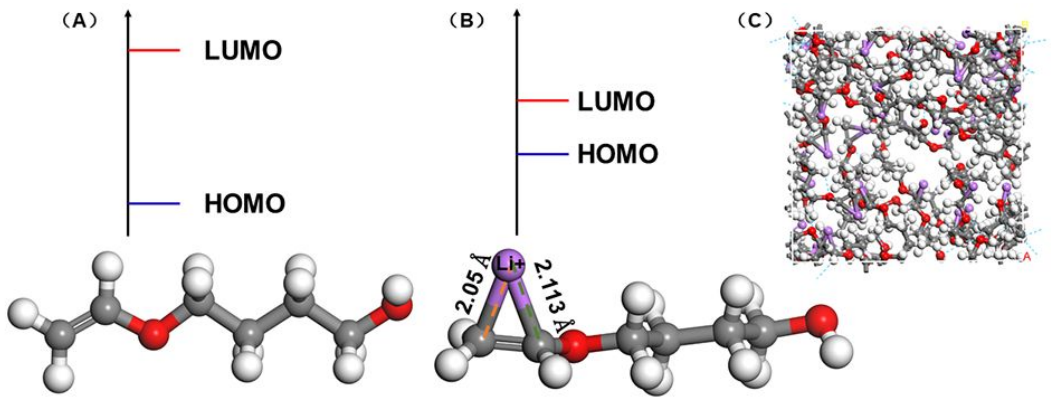

Figure S5. DFT calculations of HUMO-LUMO energy gap and hydrogen bonding in the unit cell box. (A) For pure HBVE system, the HUMO-LUMO energy gap is 5.08658 eV; (B) For $Li^{+}\cdots$VEs system, the HUMO-LUMO energy gap is 0.67861 eV; (C) Calculation of PHBVE brush conformation and hydrogen bond distribution within the observable range of AFM tip (2 nm^2).

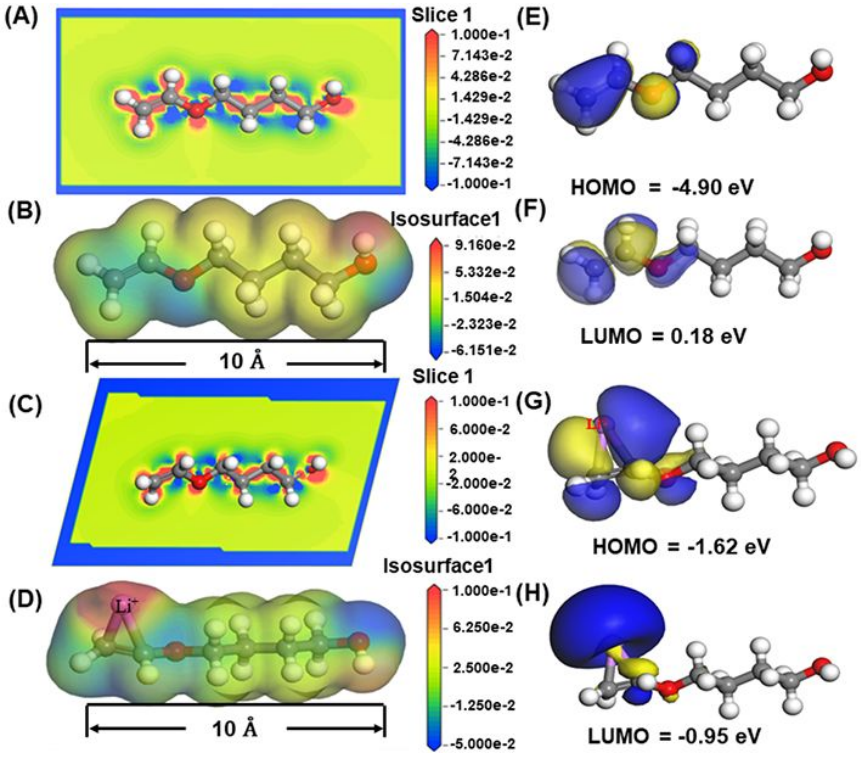

Figure S6. DFT calculations of molecular modeling, HUMO-LUMO energy and projected density of states (PDOS), all modeling and calculations are completed by MS software, the geometries of the different systems were optimized at the B3LYP level of theory. (A, B) The slice and iso-surface diagrams of PDOS of the HBVE; (C, D) The slice and iso-surface diagrams of PDOS of the $Li^{+}\cdots$HBVE; (E, F) HUMO-LUMO energy of HBVE; (G, H) HUMO-LUMO energy of $Li^{+}\cdots$HBVE.

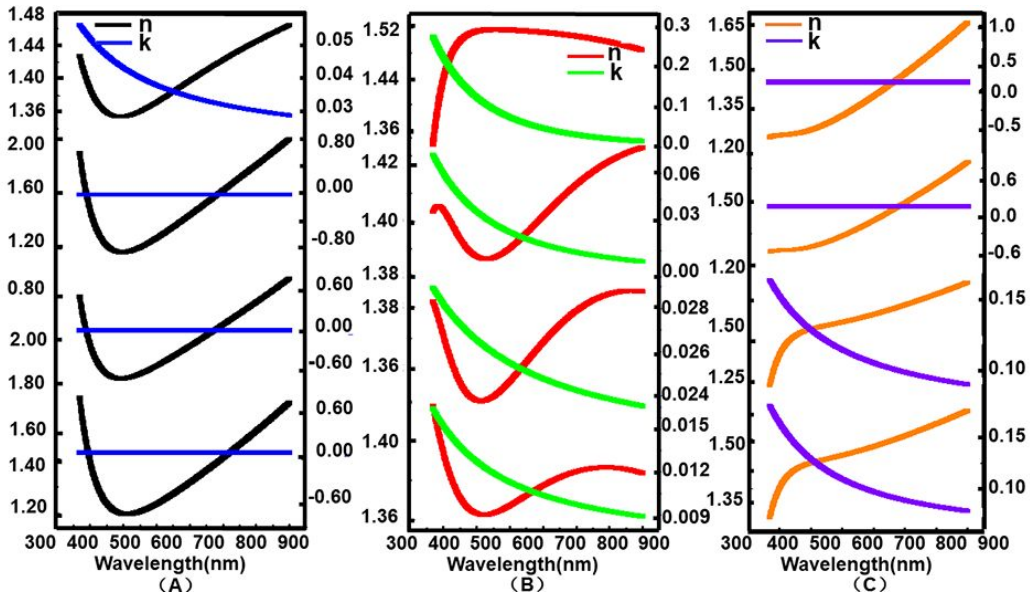

Figure S7. In-situ ellipsometry characterization of blank Si_xN_4 (A), Si_xN_4-*g*-PHBVE (RAFT, B), Si_xN_4-*g*-PHBVE (Li^+, C). Fit the thickness of the polymer brush layer according to the changes in surface refractive index "n" and extinction coefficient "k" before and after grafting.

Li^+ Catalyzed Reactions.

Research has shown that the rates of the clock rearrangements can be influenced by complexation with ions.[1] Herein, DFT calculation was performed to investigate the influence of Li^+ on π system and the mechanism of its catalyzing free radical reaction. The results suggested that an intermolecular frontier-orbital hybridization of $Li^{+}\cdots C{=}C$ occurs, leading to a new set of occupied bonding and empty antibonding orbitals, which further enormously reduced HOMO−LUMO energy gap (**Figure S5** and **Figure S6**, for pure HBVE system, the HUMO-LUMO energy gap is 5.08 eV while for $Li^{+}\cdots$VEs system, the HUMO-LUMO energy gap is 0.68 eV), providing a better prospect for transfer of electrons within a given system.[2] This mechanism also implied that a heterogeneous distribution of DOS appeared between π-π stacking segments due to the complexation of Li^+ **(Figure S6(A-D))**, as a consequence of low-energy tail states extend far into the bandgap, thus, this spatial charge-transfer generally gave rise to high reactivity of vinyl monomers. Additionally, considering that Li^+ complexation will produce a certain polarization, more or less affecting the conformation of VEs, hence, an analytical Gaussian model was expressed as a function of the molecular size, d, as shown in **Figure S6(A-D)**, the diameter of $Li^{+}\cdots$VEs complex was about 10 Å, slightly larger than VEs monomer. This suggests that the small Li^+ attached on C=C only weakly, almost has no effect on molecular morphology, but exerts a strong influence on the electron distribution of π system.

REFERENCES

[1] Clark, T. Lithium cation as radical-polymerization catalyst. *J. Am. Chem. Soc.* **2006,** *128* (34), 11278-11285.

[2] Deglmann, P.; Schäfer, A.; Lennartz, C. Application of quantum calculations in the chemical industry—An overview. *Quan. Chem.* **2015**, *115* (3),107-136.

[3] Karki, A.; Wetzelaer, G. J. A. H.; Reddy, G. N. M.; Nadazdy, V.; Seifrid, M.; Schauer, F.; Bazan, G. C.; Chmelka,

B. F.; Blom, P. W. M.; Nguyen, T. Q., Unifying energetic disorder from charge transport and band bending in organic semiconductors. *Adv Funct Mater* **2019,** *29* (20), 1901109.